Alpha-synuclein pre-formed fibrils injected into prefrontal cortex primarily impact cortical and subcortical structures and lead to restricted behavioral impacts

Matthew A. Weber, PhD[1], Gemma de Choisy[1], Ramasamy Thangavel, PhD[1], Mackenzie M. Conlon[2], Hisham A. Abdelmotilib, MD, PhD[1], Oday Halhouli, MD[1], Qiang Zhang, MD[1], Joel C. Geerling MD, PhD[1], Nandakumar S. Narayanan, MD, PhD[1], Georgina M. Aldridge, MD, PhD[#,1]

Affiliations:
[1] Department of Neurology, Roy J. and Lucille A. Carver College of Medicine, University of Iowa, Iowa City.

[2]Medical Scientist Training Program, Roy J. and Lucille A. Carver College of Medicine, University of Iowa, Iowa City.

Funding: This work was supported by NIH R01s MH116043, NS120987 to NSN and NIH K08 NS109287 and the Iowa Neuroscience Institute to GMA. This work was also supported by NIH P20NS123151 to NSN and GMA.

Conflict of Interest:
There are no conflicts of interest.

Abstract: 162
Main Text: 4647
Figures: 5
Tables: 0

Corresponding Author
Georgina M. Aldridge
georgina-aldridge@uiowa.edu
169 Newton Road
Pappjohn Biomedical Discovery Building
University of Iowa, Iowa City, 52242

Abstract

Parkinson's disease dementia (PDD) and Lewy Body dementia (LBD) are characterized by diffuse spread of alpha-synuclein (α-syn) throughout the brain. These patients have a neuropsychological pattern of deficits that include executive dysfunction, including abnormalities in planning, timing, working memory, and behavioral flexibility. The prefrontal cortex (PFC) plays a major role in normal executive function and often develops α-syn aggregates in LBD and PDD. To investigate the consequences of α-syn pathology in the cortex, we injected human α-syn pre-formed fibrils into the PFC of wildtype mice. We report that PFC PFFs: 1) induced α-syn deposition in multiple cortical and subcortical regions with sparse aggregation in midbrain and brainstem nuclei; 2) did not affect interval timing or working memory but did mildly alter behavioral flexibility as measured by reversal learning; 3) increased open field exploration; and 4) did not affect susceptibility to an inflammatory challenge. This model of cortical-dominant pathology adds to our understanding of the etiology of varied symptoms in PDD and LBD.

Key Words: Prefrontal cortex, Pre-formed fibrils, Alpha-synuclein, Behavioral flexibility, Exploration

INTRODUCTION

Patients with brainstem alpha-synuclein (α-syn) pathology have motor characteristics of Parkinson's disease (PD), including rigidity, bradykinesia, and tremor (Braak et al., 2003). However, patients with PD dementia (PDD) and Dementia with Lewy Body (DLB), collectively termed Lewy Body Dementias (LBD) have diffuse spread of α-syn throughout the brain, including cortical regions (Irwin et al., 2013; McKeith et al., 2017). These patients often suffer from severe symptoms, including executive and working memory deficits, fluctuations in arousal and attention, hallucinations and psychosis, and increased risk for delirium (FitzGerald et al., 2019; Lawson et al., 2019; McKeith et al., 2017). It is not known whether the spread of α-syn to the cortex causes the symptoms of dementia, such as impaired cognition, or whether the α-syn simply reflects a more general process of spread that does not directly affect cortical and cognitive function. To date, there are very few effective therapies approved to manage the debilitating cognitive symptoms of dementia (Halhouli et al., 2022; Zhang et al., 2020); thus, it is critical that we understand the etiological factors of the diverse symptoms seen in LBD.

To investigate the impact of cortical-predominant pathology, we induced α-syn aggregation using human pre-formed fibrils injected in the prefrontal cortex (PFC) of wild-type mice, which can induce aggregation of native α-syn that resembles the pathology described in PDD and LBD (S. Kim et al., 2019; Luk et al., 2009, 2012; Volpicelli-Daley et al., 2011). Prior literature has extensively studied both mouse and human α-syn injected in the rodent striatum, the predominant model currently used primarily due to its unique ability to induce cell loss in the substantia nigra (Luk et al., 2012; Milanese et al., 2018). A few studies have used varying initiation points, including duodenal, pedunculopontine nucleus, nucleus accumbens, olfactory bulb, and others (Ayers et al., 2018; Challis et al., 2020; Henrich et al., 2020; Rahayel et al., 2022; Rey et al., 2016, 2018; Uemura et al., 2021). These studies have offered mixed results regarding behavioral deficits and often restrict analyses to 6–7 months post-injection (mpi). Furthermore, only a few studies have investigated PFC PFF injections (Espa et al., 2019; Peeraer et al., 2015; Zhang et al., 2021). A prior report from our group found no behavioral effects of PFC PFFs;

however, these animals had a combined viral overexpression/PFF expression strategy, aged animals to 15 months (6 mpi), and only examined interval timing, novel object recognition, and open field behavior (Zhang et al., 2021). In this study, we investigated the effect of PFC PFFs on cortical, subcortical, midbrain, and brainstem α-syn pathology in mice aged up to 2 years (21 mpi) with a broader range of behavioral assays and challenges.

We report four results: 1) PFF injected in the PFC caused a consistent pattern of moderate-to-severe pathological α-syn aggregation in cortical and subcortical regions with sparse aggregation in midbrain and brainstem nuclei; 2) cognitive behaviors were mildly affected in mice with PFC PFFs, with no change in interval timing or working memory but a small, consistent alteration in behavioral flexibility as measured by reversal learning; 3) mice with cortical PFFs showed greater exploration of the center of an open field, without a change in total distance traveled; 4) mice with cortical PFFs did not have enhanced susceptibility to a delirium-like trigger. Together, these data suggest that aggregation of α-syn in cortical regions impacts specific behaviors even in the absence of midbrain/brainstem inclusion. These results provide insight into cortical synucleinopathy, which is relevant for PDD and DLB.

MATERIALS AND METHODS

Mice: All experimental procedures were performed in accordance with relevant guidelines by the University of Iowa Institutional Animal Care and Use Committee (IACUC). Wild-type male C57BL/6 mice were received from Jackson Labs (Bar Harbor, ME) at approximately 8–10 weeks of age and acclimated to the animal holding facility for 1–2 weeks. All mice were communally housed on a 12-hour light/dark cycle with *ad lib* access to standard laboratory chow and water, except as noted.

Monomer and fibril preparation: Monomeric alpha-synuclein and human pre-formed fibrils (PFFs) were a contribution from Dr. Andrew West and prepared according to previously used protocols (Abdelmotilib et al., 2017; Zhang et al., 2021). On the day of surgery, aliquoted monomers and PFFs were thawed and kept on ice immediately prior to surgical procedures. Potentially contaminated surfaces were then thoroughly cleaned with 10% bleach.

Surgical Procedures: Mice were anesthetized under 4.0% isoflurane and surgical levels of isoflurane (1.5–3.0%) were sustained for the duration of the surgery (SomnoSuite, Kent Scientific, Torrington, CT, USA). Analgesic (carprofen) and local anesthetic (bupivacaine) were administered prior to the start of surgery. An incision was made along midline and bilateral burr holes drilled above the prefrontal cortex (PFC), and a Hamilton syringe was lowered to the target coordinates (AP +1.8, ML ±0.5, DV -1.5). Mice were assigned to either bilateral microinjections of 2 µL monomers or bilateral microinjections of 2 µL PFFs. Monomeric controls or fibrils were infused over 10 minutes (0.1 µl/min; Legato 130 Syringe Pump, kd Scientific, Holliston, MA, USA), with a 5-minute wait period before removing the needle. The incision was then sutured, and mice were moved to a clean cage with *ad lib* access to food and water. Behavioral testing began approximately 10 months later.

Interval Timing Switch Task: All mice were trained to perform an interval timing switch task described in detail previously (Balci et al., 2008; Bruce et al., 2021; Larson et al., 2022; Weber et al.,

2022). Interval timing behavior was assessed on two occasions: 1) 12 mpi; 2) 20 mpi. Briefly, mildly food-restricted mice are trained in standard operant chambers (MedAssociates, St. Albans, VT) equipped with two nosepoke response ports (left and right) flanking a reward hopper and another nosepoke response port on the back wall. Either the left or right nosepoke was designated for short trials and the contralateral nosepoke for long trials (counterbalanced across mice and experimental groups). Trials are initiated by a response at the back nosepoke, which generated identical cues for both the left and right nosepokes. In short trials, mice receive a reward for the first response after 6 seconds. In long trials, mice receive a reward for the first response after 18 seconds. Because cues are identical for both short and long trials, the optimal strategy is to start responding at the short nosepoke and switch to the other nosepoke to receive a reward if enough time passed without reward.

Rapid reversal Barnes maze: A modified Barnes maze was used to evaluate acquisition and behavioral flexibility at 21 mpi using a modified Barnes maze adapted from established protocols (Gawel et al., 2019; O'Leary & Brown, 2013), with the following notable exceptions: 1) the spatial target was changed every day to a new random location and every 4 trials to an opposite location in order to assess rapid acquisition of a spatial target (first 4 trials) and reversal learning (last 4 trials); 2) to minimize the use of olfactory cues, every hole was equipped with its own 3D printed escape box "shuttle" such that no shuttle was ever re-used during a session, and the maze itself was also rotated. A plastic grate made of identical material prevented entry to incorrect shuttles; 3) following a correct response (entry), the shuttle was connected by tunnel with the home cage as a potent reward, during a 3-minute inter-trial interval. 4) a 40-hole circular Barnes maze apparatus was used in which only 10 holes were available. This protocol was done for 3 consecutive days. Total distance traveled was captured with overhead cameras and analyzed using ANYMaze 7.14d (Stoelting, Wood Dale, IL).

Open field: Open field was used to assess exploration and activity levels on two occasions (12- and 16 mpi), using methods described previously (Kraeuter et al., 2019; Tatem et al., 2014). On each

occasion, mice were habituated to behavior rooms for at least 30 minutes prior to testing. Mice were placed in the center of an empty open field arena (40 cm × 40 cm × 30 cm) and allowed to explore uninterrupted for 10 minutes. Mice were returned to their home cage immediately, and the open field arenas were thoroughly cleaned with 70% ethanol and allowed to air dry between trials. Rescue disinfectant (0.5% hydrogen peroxide) was used between cohorts. Total distance traveled and thigmotaxis (distance traveled outside a 25.5 × 25.5 cm central square divided by total distance traveled) were analyzed using ANYMaze 7.14d.

Home cage activity: Home cage activity was assessed in parallel with nest building and food burrowing (described below) at 15 mpi. Overhead cameras captured morning and nighttime activity using an infrared camera. AnyMaze 7.14d software was then used to quantify periods of activity and rest over a one-hour period during the morning (~6–7 am) and night (~2–3 am). Midday activity could not be quantified due to unexpected interference with lighting through cage bars. Periods of immobility were defined as periods 40-seconds or longer during which AnyMaze did not detect movement. Percent immobile was then defined as the number of seconds the mouse spent immobile compared with total seconds tracked. Bout length was based on prior published data using EEG suggesting that periods of immobility greater than 40-seconds are likely to be sleep bouts (Fisher et al., 2012).

Nesting: Nest building was used to approximate general health and welfare, using slightly modified methods described previously (Neely et al., 2019). Nesting behavior for each mouse was assessed on two occasions (15- and 16 mpi). At 15 mpi, three different materials (shredded paper, paper twist, and pressed cotton square) were provided on separate days. At 16 mpi, only the paper nest building material was provided. Photographs were taken of each nest and scored by blinded observers on a scale of 1–5 according to previous literature (Gaskill et al., 2013; Neely et al., 2019).

Food burrowing: Food burrowing was assessed in parallel with nest building at 16 mpi. Pre-weighed food was provided in a glass jar equipped with a PLA 3D printed cone-shaped hopper to prevent mice from nesting in the jar. The jar was weighed the following day to calculate food burrowed or eaten.

Lipopolysaccharide injection challenge: Systemic infection increases risk of developing delirium and dementia in humans (Matsuo et al., 2017; Quispel□Aggenbach et al., 2021; Spiller & Keen, 2006)and peripheral injections of lipopolysaccharide (LPS) are widely used as a model of systemic infection and resultant behavioral changes in rodents (Culley et al., 2014; Field et al., 2012; Luk et al., 2009; Sparkman et al., 2006). At 16 mpi, 0.5 mg/kg LPS (Sigma #L2880, St. Louis, MO) diluted in 0.9% sterile saline was injected intraperitoneally (ip.) in five mice with PFC monomers and five mice with PFC PFFs. The remaining three mice with PFC monomers and three mice with PFC PFFs were injected with equivalent volumes of saline. Behavior in the open field, food burrowing assay, and nest building was then assessed.

Histology: Mice were anesthetized with ketamine (100 mg/kg ip.) and xylazine (10 mg/kg ip.) and transcardially perfused with phosphate-buffered saline (PBS) and 4% paraformaldehyde (PFA). Brains were fixed in 5% PFA overnight and immersed in 30% sucrose for approximately 48 hours. Brains were then serially sliced into 40-μm coronal sections using a cryostat (Leica Biosystems, Deer Park, IL). Brain sections were blocked for one hour in 2% normal goat serum (NGS) in PBST (0.3% Triton X-100 in 1x PBS) and then incubated for approximately 20 hours at 4°C in either rabbit anti-α-synuclein phosphorylated serine 129 (Abcam #EP1536Y, Cambridge, United Kingdom) diluted to 1:1000 in blocking solution or rabbit anti-tyrosine hydroxylase (TH; Millipore #AB152, Burlington, MA) diluted to 1:1000 in blocking solution. Sections were then washed in PBS three times and incubated overnight at 4°C in goat anti-rabbit IgG (H+L) Alexa Fluor 647 secondary antibody (Invitrogen #A11036, Waltham, MA) diluted to 1:1000 in blocking. Sections were washed three more times. To stain for nissl, sections were washed in PBST for 10 minutes and two additional 5-minute washes in PBS. Sections were

incubated in NeuroTrace™ 435/455 (Thermo Fisher Scientific Inc. #N21479, Waltham, MA) diluted 1:300 in PBS for 20 minutes at room temperature and then washed in PBST for 10 minutes and twice in PBS for 5 minutes each. After one more wash at room temperature for 2 hours, sections were mounted with ProLong Diamond Antifade Mountant (Invitrogen #P36961) on Superfrost microscope slides (Fisher Scientific).

All sections were imaged using VS-ASW-S6 imaging software (Olympus, Center Valley, PA) and an Olympus Slide Scanner (Olympus VS120) with a 20x objective. To characterize pathological spread of α-synuclein, we semi-quantitively graded the degree of P-S129 inclusions in multiple regions of interest (ROI; see Fig. 2 for complete list) referenced from Franklin & Paxinos, 2008. The α-syn pathology was graded based on prior literature (Rey et al., 2019). Briefly, pathology was assigned on a scale of 0–4; 0: no soma or neurite P-S129 positive staining; 1: sparse/light soma or neurite staining (1–3 somas or neurites per 750 µm square area with ROI); 2: mild burden (4 or more somas or neurites per 750 µm, with definitive areas showing no P-S129 staining); 3: dense burden (>10 soma or neurites per 250 µm); 4: heavy burden (>20 somas or neurites per 250 µm). For every brain, one out of every six 40 um sections were graded for α-syn inclusion. Regions of interest were quantified and results averaged, even for sections that contained no pathology.

Statistics: All data was analyzed using custom written Matlab routines and Graphpad Prism. For interval timing and open field at 12 mpi, we analyzed the effects of PFFs injected in the PFC with unpaired t-tests. For interval timing behavior, after behavioral acquisition, three-to-four sessions were collected, and switch time coefficient of variability and mean switch times were analyzed. For open field behavior, total distance (in meters) and thigmotaxis was analyzed. For home cage activity at 18 mpi, we used mixed-effects two-way analysis of variance (ANOVA). Note that one mouse from each group was excluded from the daytime test due to unexpected interference with lighting and tracking. For nest building at 18 mpi, we used separate non-parametric Wilcoxon ranksum tests for each material. For LPS-challenge, groups were compared using two-way ANOVA with LPS and PFF as main effects (open field

distance and thigmotaxis) or using three-way ANOVA with LPS, PFF, and time as main effects (food burrowing). Nest building was compared using multiple non-corrected Wilcoxon ranksum tests. For all behavioral tests done at the post-LPS time-points, evaluation was first done using prior LPS as an interaction variable. However, as no significant effect of prior LPS effect was observed, data was collapsed to compare monomer control and PFF groups irrespective of prior LPS exposure.

For striatal α-syn aggregation, subregions were compared using one-way repeated measures ANOVA followed by Tukey's post-hoc test for multiple comparisons. For tyrosine hydroxylase positive (TH+) fluorescence, we used separate unpaired t-tests to compare levels of arbitrary fluorescent units for each of the regions sampled (PFC, striatum, ventral tegmental area, substantia nigra).

RESULTS

Pathology

Injections of PFFs in the PFC led to α-syn aggregation in the targeted cortical area as well as several downstream regions. We found clear and dense pathological spread of α-syn in orbitofrontal, secondary motor M2, perirhinal, entorhinal, piriform, nucleus accumbens, amygdala, and thalamus (Fig. 2C-D). Subregions of the striatum were differentially affected by PFFs injected in the PFC (Fig. 2F). There was a statistically significant difference in α-syn aggregation between subregions of the striatum ($F_{(1.646, 11.52)} = 32.07$, $p < 0.0001$). Post-hoc analyses revealed the densest aggregation in the dorsomedial striatum (vs. dorsolateral ($p < 0.0001$), ventromedial ($p < 0.05$), ventrolateral ($p < 0.0001$)). Further, both dorsolateral and ventromedial subregions contained denser α-syn aggregation than ventrolateral striatum ($p < 0.01$ and $p < 0.05$, respectively). However, unlike other subcortical regions, subregions of the hippocampus were considerably less dense. Similar sparse-to-absent pathological α-syn aggregation was observed in regions of the midbrain and brainstem.

We also quantified tyrosine hydroxylase positive (TH+) fluorescence levels in the PFC, striatum, ventral tegmental area, and substantia nigra (Fig. 2G), similar to prior methods established in the lab (Weber et al., 2022). We found no significant change in TH+ fluorescent levels in PFF-injected mice compared with controls in any of the four regions: PFC ($t(14) = 0.38$; $p = 0.71$), striatum ($t(14) = 0.07$; $p = 0.99$), ventral tegmental area ($t(14) = 0.57$; $p = 0.58$), and substantia nigra ($t(14) = 0.10$; $p = 0.92$).

Cognitive behaviors: Interval timing and behavioral flexibility

Interval timing requires mice to estimate an interval of several seconds and requires working memory for temporal rules as well as attention to the passage of time. Our prior work showed no deficits in interval timing using a fixed-interval timing task at 15 months of age (6 mpi of PFFs). We used an interval timing switch task, which enables us to track mean temporal estimates as well as the variability of temporal estimates. We found that at 12 mpi, mice injected with PFFs showed no difference in mean

switch times (shifting early or late as an estimate of timing accuracy; Fig. 3A; $t(13) = 0.66$; $p = 0.52$) and no difference in switch time coefficient of variability (estimate of timing precision; Fig. 3B; $t(13) = 1.05$; $p = 0.31$). One PFF injected mouse was excluded as a result of no trials initiated or rewards obtained, likely due to a lack of motivation to perform the task. We repeated interval timing switch task training at 20 mpi. Two monomer-treated mice were sacrificed at 19 mpi due to age-related health concerns, so this round of interval timing training included six monomer and eight PFF mice. Similar to interval timing at 12 mpi, we found no difference in mean switch times (Fig. 3C; $t(12) = 0.29$; $p = 0.78$) or the coefficient of variability of switch times (Fig. 3D; $t(12) = 1.20$; $p = 0.25$). These results suggest that PFC PFFs do not affect interval timing behavior even at 20 mpi.

After interval timing training, two mice treated with PFFs were sacrificed due to age-related health concerns. Therefore, six monomer and six PFF mice remained. To test learning and behavioral flexibility, all remaining mice were tested using rapid reversal Barnes maze at 21 mpi. PFF mice showed an altered pattern of behavior flexibility, with PFF mice learning quickly during the initial trials, but then travelling a greater distance to reach the target compared with control mice during the reversal phase (Fig. 3E; main effect of trial ($F_{(2.145, 19.31)} = 6.71$; $p < 0.01$) and trial × treatment interaction ($F_{(7,63)} = 2.17$; $p < 0.05$); post-hoc analyses revealed no significant differences when corrected for multiple-comparisons).

Open field

We assessed exploration and activity levels in the open field. At 12 mpi, mice injected with PFFs in the PFC did not differ from monomer controls in distance traveled (meters) over the 10-minute test (Fig. 4A; $t(13) = 0.39$; $p = 0.71$), but did display reduced thigmotaxis, showing more exploration of the center of the arena (Fig. 4B; $t(13) = 2.36$; $p < 0.05$). These results may suggest greater exploration or reduced anxiety-like behavior.

Home cage activity and nest building (15 mpi)

To assess general health and welfare as well as naturalistic behaviors, we used assays to examine home cage activity and nest building. At 15 mpi, mice injected with PFFs in the PFC did not differ on amount of home cage activity during either the light or dark cycle (Fig. 4C; main effect of treatment $F_{(1, 14)} < 0.05$; $p = 0.84$), but there was a significant main effect of time of day ($F_{(1, 12)} = 50.45$; $p = < 0.0001$). At the same time-point, there were no differences in nest building score across three different types of material (Fig. 4D; paper Wilcoxon $p = 0.61$; twist Wilcoxon $p = 0.42$; squares Wilcoxon $p = 0.18$). Altogether, these data suggest that PFC PFFs do not reduce naturalistic innate behaviors or overall well-being.

Peripheral immune activation (16 mpi)

We tested if mice previously injected with PFF were more susceptible to peripheral immune activation by lipopolysaccharide (LPS) injections. At 16 mpi, we injected five mice with PFC PFFs and five mice with PFC monomers with 0.5 mg/kg LPS. The remaining three mice in each group received equivalent volumes of saline. We then tested behavior in the open field, food burrowing, and nest building assays. Although LPS caused a significant decrease in distance travelled (Fig. 5A; $F_{(1, 12)} = 44.82$; $p = < 0.0001$) and food burrowing ($F_{(1, 12)} = 25.64$; $p = < 0.001$), we found no evidence of an enhanced response in PFF injected mice (Fig. 5A; distance travelled $F_{(1, 12)} = 1.33$; $p = 0.27$; Fig. 5B; thigmotaxis $F_{(1, 11)} = 0.52$; $p = 0.49$; Fig. 5C; food burrowing $F_{(1, 12)} = 1.32$; $p = 0.27$). Unlike 12 mpi, there was no significant effect of PFFs on thigmotaxis ($F_{(1, 11)} = 2.46$; $p = 0.15$), possibly due to a lack of statistical power, as the pattern remained similar. There was also no enhanced response in the nest building assay as well (1-day post LPS injection Wilcoxon $p = 0.16$). These data suggest that PFC PFF mice are not more susceptible to peripheral immune activation.

DISCUSSION

We tested the effects of prefrontal cortex (PFC) pre-formed fibrils (PFFs) in aged mice on a range of behavioral assays. First, we found that PFC PFF injection triggered widespread cortical and subcortical α-synuclein (α-syn) aggregation, without significant spread to brainstem regions, allowing evaluation of the behavioral impact of α-syn limited to these regions. Second, and in line with our prior work, we found no reliable deficits in interval timing, but we did find mild deficits in reversal learning. Third, we also found changes in exploration without changes in distance travelled in the open field assay. Finally, we found no effects of inflammatory challenge. Taken together, these data help establish the validity of mouse models of cortical PFFs, which might be of great value for efforts investigating basic mechanisms of synucleinopathies such as PDD and LBD.

Notably, prior work from our group has shown that human PFFs injected in the PFC does not affect interval timing or open field behavior 6 mpi in mice aged 15 months (Zhang et al., 2021). Prior work from our group and others has shown that people with Parkinson's disease display reliable deficits in interval timing (Kim et al., 2017; Malapani et al., 1998; Pastor et al., 1992; Singh et al., 2021) and that the PFC is crucial for interval timing behavior (Kim et al., 2017; Parker et al., 2015). The data presented here, and our prior report demonstrate that PFC PFFs are not sufficient to affect interval timing. This may because midbrain dopaminergic cell loss, which is absent in this model, may be necessary for interval timing deficits (Kim et al., 2017; Weber et al., 2022).

While α-syn aggregates were widespread and dense in cortical and subcortical regions, mice that received PFC PFF injections displayed only mild behavioral deficits. First, we found that PFF mice did not display any difference in measures of interval timing, including variability of or mean switch times. This result in is line with prior work from our group (Zhang et al., 2021) and suggests that PFC PFFs and the resulting α-syn aggregation is not sufficient to induce an interval timing deficit, even up to 20 mpi. We also found that PFF mice displayed reduced thigmotaxis at 12 mpi, with the same non-significant pattern observed at 16 mpi, which may suggest a difference in explorative and anxiolytic behaviors in the open field as a result of PFC PFF injections. Further, we also found that PFF mice learned quickly, but

required a longer search route to locate the target exit hole during the reversal phase of a daily spatial training Barnes maze task at 21 mpi, suggesting altered behavioral flexibility.

The rodent PFC is a highly connected brain region, sending projections to multiple cortical, subcortical, midbrain, and brainstem nuclei (Anastasiades & Carter, 2021; Souza et al., 2022). Our prior work suggested that human PFFs injected into PFC cause a consistent but limited pattern of α-syn pathology including PFC, temporal cortex, and striatum. The consequences of α-syn outside of the brainstem, as occurs in LBD, are still relatively unknown. Using this model helps tease out the consequences of cortical/subcortical α-syn pathology in the absence of dramatic loss of neurons in brainstem regions. Using semi-quantitative analysis of 25 brain regions, we demonstrate dense pathological spread of α-syn in multiple cortical regions such as the orbitofrontal, secondary motor M2, perirhinal, entorhinal, and piriform. A consistent pattern of α-syn was also observed in subcortical regions, including the striatum, nucleus accumbens, amygdala, and thalamus. We note that there is differential expression of α-syn in subregions of the striatum, matching the direct connectivity of our prefrontal injection-site, in line with prior work from Gabbott and colleagues (2005). We targeted the dorsal prelimbic and anterior cingulate subregions of the PFC, which contain a greater number of neurons that project to the dorsal striatum compared to the ventral prelimbic and infralimbic subregions of the PFC that contain more ventral striatal projecting neurons. We also note that, unlike other subcortical regions, the subregions of the hippocampus were relatively spared from α-syn aggregation. This finding was again in line with prior literature suggesting that cortical input to the hippocampus passes through the perirhinal and entorhinal cortices first (Burwell & Amaral, 1998), two areas that show dense α-syn deposition here. While there was clear α-syn in cortical and subcortical regions, we found little or no α-syn pathology in midbrain and brainstem nuclei, including substantia nigra, locus coeruleus, and dorsal raphe. Together, these findings extend our prior work to show that the aggregation induced in cortical and subcortical regions by human PFFs injected into PFC are not cleared over the course of aging, as has been reported in some brain regions (Sun et al., 2022).

This study has several limitations. First, our control animals received monomer injections, which has been shown previously to lead to mild and transient aggregation (Manfredsson et al., 2018). We did note some mild p-syn positive puncta, but morphology was distinct and punctate, and may have been caused by aging alone. Fibrillar and “lewy-neurite-like” structures were only seen in PFF injected mice, and this was confirmed by confocal microscopy. Second, we did not include a group of young mice to determine whether our lack of behavioral change was primarily due to age-related decline in cognitive function or interval timing, which has been observed previously (Beas et al., 2017; Gür et al., 2020), although the interval timing behavior presented here is similar to previously published work from our group using healthy, young C57BL/6 mice (Bruce et al., 2021). Third, our measures of interval timing and behavioral flexibility do not fully interrogate cognitive dysfunctions related to PDD and LBD and it is possible that other cognitive behaviors such as attention or impulse control were negatively affected by PFC PFF injections. Fourth, behavioral experiments at the later timepoints are underpowered to detect subtle differences due to age-related loss. However, due to careful pathological confirmation of each mouse in this two-year study, we believe these results inform future research and are important for understanding this model. Finally, this study was limited to male mice. Recent evidence suggest female mice may show reduced pathology compared with male mice (Gezer, 2020). Human males are more likely to be diagnosed with PD and LBD (Savica et al., 2013; Van Den Eeden, 2003; Wooten, 2004). Understanding potential differences in pathology due to sex is an essential goal of future research and fully powered studies of both sexes are needed.

In summary, our results describe widespread cortical and subcortical α-syn aggregation from PFC PFFs with mild behavioral alterations that were not modulated by an inflammatory challenge. The lack of brainstem involvement is notable and could provide insight into the brain networks that drive behavioral deficits in PD, PDD, and DLB.

ACKNOWLEDGMENTS

This work was supported by NIH R01s MH116043, NS120987 to NSN and NIH K08 NS109287 and the Iowa Neuroscience Institute to GMA. We thank Dr. Andrew West for generously providing the pre-formed fibrils and Travis Larson for assisting with behavioral experiments.

DATA AVAILABILITY

All raw data are available at https://aldridge.lab.uiowa.edu/open-science.

CODE AVAILABILITY

All code is available at https://aldridge.lab.uiowa.edu/open-science.

AUTHOR CONTRIBUTIONS

MAW, HA, QZ, NSN, and GMA designed the animal experiments. MAW, MMC, HA, GdC, OH, and GMA performed all experiments. GdC, RT, and JG performed histological analyses. MAW and GMA performed all statistical analyses. MAW and GMA wrote the manuscript, and all authors reviewed and revised the manuscript.

COMPETING INTERESTS

The authors declare that there are no conflicts of interest.

REFERENCES

Abdelmotilib, H., Maltbie, T., Delic, V., Liu, Z., Hu, X., Fraser, K. B., Moehle, M. S., Stoyka, L., Anabtawi, N., Krendelchtchikova, V., Volpicelli-Daley, L. A., & West, A. (2017). α-Synuclein fibril-induced inclusion spread in rats and mice correlates with dopaminergic Neurodegeneration. *Neurobiology of Disease*, *105*, 84–98. https://doi.org/10.1016/j.nbd.2017.05.014

Anastasiades, P. G., & Carter, A. G. (2021). Circuit organization of the rodent medial prefrontal cortex. *Trends in Neurosciences*, *44*(7), 550–563. https://doi.org/10.1016/j.tins.2021.03.006

Ayers, J. I., Riffe, C. J., Sorrentino, Z. A., Diamond, J., Fagerli, E., Brooks, M., Galaleldeen, A., Hart, P. J., & Giasson, B. I. (2018). Localized Induction of Wild-Type and Mutant Alpha-Synuclein Aggregation Reveals Propagation along Neuroanatomical Tracts. *Journal of Virology*, *92*(18), e00586-18. https://doi.org/10.1128/JVI.00586-18

Balci, F., Papachristos, E. B., Gallistel, C. R., Brunner, D., Gibson, J., & Shumyatsky, G. P. (2008). Interval timing in genetically modified mice: A simple paradigm. *Genes, Brain and Behavior*, *7*(3), 373–384. https://doi.org/10.1111/j.1601-183X.2007.00348.x

Beas, B. S., McQuail, J. A., Bañuelos, C., Setlow, B., & Bizon, J. L. (2017). Prefrontal cortical GABAergic signaling and impaired behavioral flexibility in aged F344 rats. *Neuroscience*, *345*, 274–286. https://doi.org/10.1016/j.neuroscience.2016.02.014

Braak, H., Tredici, K. D., Rüb, U., de Vos, R. A. I., Jansen Steur, E. N. H., & Braak, E. (2003). Staging of brain pathology related to sporadic Parkinson's disease. *Neurobiology of Aging*, *24*(2), 197–211. https://doi.org/10.1016/S0197-4580(02)00065-9

Bruce, R. A., Weber, M. A., Volkman, R. A., Oya, M., Emmons, E. B., Kim, Y., & Narayanan, N. S. (2021). Experience-related enhancements in striatal temporal encoding. *The European Journal of Neuroscience*, *54*(3), 5063–5074. https://doi.org/10.1111/ejn.15344

Burwell, R. D., & Amaral, D. G. (1998). Cortical afferents of the perirhinal, postrhinal, and entorhinal cortices of the rat. *The Journal of Comparative Neurology*, *398*(2), 179–205. https://doi.org/10.1002/(SICI)1096-9861(19980824)398:2<179::AID-CNE3>3.0.CO;2-Y

Challis, C., Hori, A., Sampson, T. R., Yoo, B. B., Challis, R. C., Hamilton, A. M., Mazmanian, S. K., Volpicelli-Daley, L. A., & Gradinaru, V. (2020). Gut-seeded α-synuclein fibrils promote gut dysfunction and brain pathology specifically in aged mice. *Nature Neuroscience*, *23*(3), 327–336. https://doi.org/10.1038/s41593-020-0589-7

Culley, D. J., Snayd, M., Baxter, M. G., Xie, Z., Lee, I. H., Rudolph, J., Inouye, S. K., Marcantonio, E. R., & Crosby, G. (2014). Systemic inflammation impairs attention and cognitive flexibility but not associative learning in aged rats: Possible implications for delirium. *Frontiers in Aging Neuroscience*, *6*, 107. https://doi.org/10.3389/fnagi.2014.00107

Espa, E., Clemensson, E. K. H., Luk, K. C., Heuer, A., Björklund, T., & Cenci, M. A. (2019). Seeding of protein aggregation causes cognitive impairment in rat model of cortical synucleinopathy. *Movement Disorders*, *34*(11), 1699–1710. https://doi.org/10.1002/mds.27810

Field, R. H., Gossen, A., & Cunningham, C. (2012). Prior Pathology in the Basal Forebrain Cholinergic System Predisposes to Inflammation-Induced Working Memory Deficits: Reconciling Inflammatory and Cholinergic Hypotheses of Delirium. *Journal of Neuroscience*, *32*(18), 6288–6294. https://doi.org/10.1523/JNEUROSCI.4673-11.2012

Fisher, S. P., Godinho, S. I. H., Pothecary, C. A., Hankins, M. W., Foster, R. G., & Peirson, S. N. (2012). Rapid Assessment of Sleep-Wake Behavior in Mice. *Journal of Biological Rhythms*, *27*(1), 48–58. https://doi.org/10.1177/0748730411431550

FitzGerald, J. M., Perera, G., Chang-Tave, A., Price, A., Rajkumar, A. P., Bhattarai, M., O'Brien, J. T., Ballard, C., Aarsland, D., Stewart, R., & Mueller, C. (2019). The Incidence of Recorded Delirium Episodes Before and After Dementia Diagnosis: Differences Between Dementia With Lewy Bodies and Alzheimer's Disease. *Journal of the American Medical Directors Association*, *20*(5), 604–609. https://doi.org/10.1016/j.jamda.2018.09.021

Franklin, K. B. J., & Paxinos, G. (2008). *The mouse brain in stereotaxic coordinates* (Compact 3. ed). Elsevier Academic Press.

Gaskill, B. N., Karas, A. Z., Garner, J. P., & Pritchett-Corning, K. R. (2013). Nest Building as an Indicator of Health and Welfare in Laboratory Mice. *Journal of Visualized Experiments*, *82*, 51012. https://doi.org/10.3791/51012

Gawel, K., Gibula, E., Marszalek-Grabska, M., Filarowska, J., & Kotlinska, J. H. (2019). Assessment of spatial learning and memory in the Barnes maze task in rodents—Methodological consideration. *Naunyn-Schmiedeberg's Archives of Pharmacology*, *392*(1), 1–18. https://doi.org/10.1007/s00210-018-1589-y

Gezer, A. O. (2020). Sex-specific Effects of Developmental Dieldrin Exposure on Synucleinopathy [Ph.D., Michigan State University]. In *ProQuest Dissertations and Theses* (2404294669). Dissertations & Theses @ CIC Institutions; ProQuest Dissertations & Theses Global.

http://login.proxy.lib.uiowa.edu/login?url=https://www.proquest.com/dissertations-theses/sex-specific-effects-developmental-dieldrin/docview/2404294669/se-2?accountid=14663

Gür, E., Duyan, Y. A., Arkan, S., Karson, A., & Balcı, F. (2020). Interval timing deficits and their neurobiological correlates in aging mice. *Neurobiology of Aging*, *90*, 33–42. https://doi.org/10.1016/j.neurobiolaging.2020.02.021

Halhouli, O., Zhang, Q., & Aldridge, G. M. (2022). Caring for patients with cognitive dysfunction, fluctuations and dementia caused by Parkinson's disease. In *Progress in Brain Research* (Vol. 269, pp. 407–434). Elsevier. https://doi.org/10.1016/bs.pbr.2022.01.018

Henrich, M. T., Geibl, F. F., Lakshminarasimhan, H., Stegmann, A., Giasson, B. I., Mao, X., Dawson, V. L., Dawson, T. M., Oertel, W. H., & Surmeier, D. J. (2020). Determinants of seeding and spreading of α-synuclein pathology in the brain. *Science Advances*, *6*(46), eabc2487. https://doi.org/10.1126/sciadv.abc2487

Irwin, D. J., Lee, V. M.-Y., & Trojanowski, J. Q. (2013). Parkinson's disease dementia: Convergence of α-synuclein, tau and amyloid-β pathologies. *Nature Reviews Neuroscience*, *14*(9), 626–636. https://doi.org/10.1038/nrn3549

Kim, S., Kwon, S.-H., Kam, T.-I., Panicker, N., Karuppagounder, S. S., Lee, S., Lee, J. H., Kim, W. R., Kook, M., Foss, C. A., Shen, C., Lee, H., Kulkarni, S., Pasricha, P. J., Lee, G., Pomper, M. G., Dawson, V. L., Dawson, T. M., & Ko, H. S. (2019). Transneuronal Propagation of Pathologic α-Synuclein from the Gut to the Brain Models Parkinson's Disease. *Neuron*, *103*(4), 627-641.e7. https://doi.org/10.1016/j.neuron.2019.05.035

Kim, Y.-C., Han, S.-W., Alberico, S. L., Ruggiero, R. N., De Corte, B., Chen, K.-H., & Narayanan, N. S. (2017). Optogenetic Stimulation of Frontal D1 Neurons Compensates for Impaired Temporal Control of Action in Dopamine-Depleted Mice. *Current Biology*, *27*(1), 39–47. https://doi.org/10.1016/j.cub.2016.11.029

Kraeuter, A.-K., Guest, P. C., & Sarnyai, Z. (2019). The Open Field Test for Measuring Locomotor Activity and Anxiety-Like Behavior. In P. C. Guest (Ed.), *Pre-Clinical Models* (Vol. 1916, pp. 99–103). Springer New York. https://doi.org/10.1007/978-1-4939-8994-2_9

Larson, T., Khandelwal, V., Weber, M. A., Leidinger, M. R., Meyerholz, D. K., Narayanan, N. S., & Zhang, Q. (2022). Mice expressing P301S mutant human tau have deficits in interval timing. *Behavioural Brain Research*, *432*, 113967. https://doi.org/10.1016/j.bbr.2022.113967

Lawson, R. A., McDonald, C., & Burn, D. J. (2019). Defining delirium in idiopathic Parkinson's disease: A systematic review. *Parkinsonism & Related Disorders*, *64*, 29–39. https://doi.org/10.1016/j.parkreldis.2018.09.025

Luk, K. C., Kehm, V., Carroll, J., Zhang, B., O'Brien, P., Trojanowski, J. Q., & Lee, V. M.-Y. (2012). Pathological α-Synuclein Transmission Initiates Parkinson-like Neurodegeneration in Nontransgenic Mice. *Science*, *338*(6109), 949–953. https://doi.org/10.1126/science.1227157

Luk, K. C., Song, C., O'Brien, P., Stieber, A., Branch, J. R., Brunden, K. R., Trojanowski, J. Q., & Lee, V. M.-Y. (2009). Exogenous α-synuclein fibrils seed the formation of Lewy body-like intracellular inclusions in cultured cells. *Proceedings of the National Academy of Sciences*, *106*(47), 20051–20056. https://doi.org/10.1073/pnas.0908005106

Malapani, C., Rakitin, B., Levy, R., Meck, W. H., Deweer, B., Dubois, B., & Gibbon, J. (1998). Coupled Temporal Memories in Parkinson's Disease: A Dopamine-Related Dysfunction. *Journal of Cognitive Neuroscience*, *10*(3), 316–331. https://doi.org/10.1162/089892998562762

Manfredsson, F. P., Luk, K. C., Benskey, M. J., Gezer, A., Garcia, J., Kuhn, N. C., Sandoval, I. M., Patterson, J. R., O'Mara, A., Yonkers, R., & Kordower, J. H. (2018). Induction of alpha-synuclein pathology in the enteric nervous system of the rat and non-human primate results in gastrointestinal dysmotility and transient CNS pathology. *Neurobiology of Disease*, *112*, 106–118. https://doi.org/10.1016/j.nbd.2018.01.008

Matsuo, N., Morita, T., Matsuda, Y., Okamoto, K., Matsumoto, Y., Kaneishi, K., Odagiri, T., Sakurai, H., Katayama, H., Mori, I., Yamada, H., Watanabe, H., Yokoyama, T., Yamaguchi, T., Nishi, T., Shirado, A., Hiramoto, S., Watanabe, T., Kohara, H., … Iwase, S. (2017). Predictors of Delirium in Corticosteroid-Treated Patients with Advanced Cancer: An Exploratory, Multicenter, Prospective, Observational Study. *Journal of Palliative Medicine*, *20*(4), 352–359. https://doi.org/10.1089/jpm.2016.0323

McKeith, I. G., Boeve, B. F., Dickson, D. W., Halliday, G., Taylor, J.-P., Weintraub, D., Aarsland, D., Galvin, J., Attems, J., Ballard, C. G., Bayston, A., Beach, T. G., Blanc, F., Bohnen, N., Bonanni, L., Bras, J., Brundin, P., Burn, D., Chen-Plotkin, A., … Kosaka, K. (2017). Diagnosis and management of dementia with Lewy bodies: Fourth consensus report of the DLB Consortium. *Neurology*, *89*(1), 88–100. https://doi.org/10.1212/WNL.0000000000004058

Milanese, C., Cerri, S., Ulusoy, A., Gornati, S. V., Plat, A., Gabriels, S., Blandini, F., Di Monte, D. A., Hoeijmakers, J. H., & Mastroberardino, P. G. (2018). Activation of the DNA damage response in

vivo in synucleinopathy models of Parkinson's disease. *Cell Death & Disease*, *9*(8), 818. https://doi.org/10.1038/s41419-018-0848-7

Neely, C. L. C., Pedemonte, K. A., Boggs, K. N., & Flinn, J. M. (2019). Nest Building Behavior as an Early Indicator of Behavioral Deficits in Mice. *Journal of Visualized Experiments*, *152*, 60139. https://doi.org/10.3791/60139

O'Leary, T. P., & Brown, R. E. (2013). Optimization of apparatus design and behavioral measures for the assessment of visuo-spatial learning and memory of mice on the Barnes maze. *Learning & Memory*, *20*(2), 85–96. https://doi.org/10.1101/lm.028076.112

Parker, K. L., Ruggiero, R. N., & Narayanan, N. S. (2015). Infusion of D1 Dopamine Receptor Agonist into Medial Frontal Cortex Disrupts Neural Correlates of Interval Timing. *Frontiers in Behavioral Neuroscience*, *9*. https://doi.org/10.3389/fnbeh.2015.00294

Pastor, M. A., Artieda, J., Jahanshahi, M., & Obeso, J. A. (1992). TIME ESTIMATION AND REPRODUCTION IS ABNORMAL IN PARKINSON'S DISEASE. *Brain*, *115*(1), 211–225. https://doi.org/10.1093/brain/115.1.211

Peeraer, E., Bottelbergs, A., Van Kolen, K., Stancu, I.-C., Vasconcelos, B., Mahieu, M., Duytschaever, H., Ver Donck, L., Torremans, A., Sluydts, E., Van Acker, N., Kemp, J. A., Mercken, M., Brunden, K. R., Trojanowski, J. Q., Dewachter, I., Lee, V. M. Y., & Moechars, D. (2015). Intracerebral injection of preformed synthetic tau fibrils initiates widespread tauopathy and neuronal loss in the brains of tau transgenic mice. *Neurobiology of Disease*, *73*, 83–95. https://doi.org/10.1016/j.nbd.2014.08.032

Quispel□Aggenbach, D. W. P., Schep□de Ruiter, E. P. R., Bergen, W., Bolling, J. R., Zuidema, S. U., & Luijendijk, H. J. (2021). Prevalence and risk factors of delirium in psychogeriatric outpatients. *International Journal of Geriatric Psychiatry*, *36*(1), 190–196. https://doi.org/10.1002/gps.5413

Rahayel, S., Mišić, B., Zheng, Y.-Q., Liu, Z.-Q., Abdelgawad, A., Abbasi, N., Caputo, A., Zhang, B., Lo, A., Kehm, V., Kozak, M., Yoo, H. S., Dagher, A., & Luk, K. C. (2022). Differentially targeted seeding reveals unique pathological alpha-synuclein propagation patterns. *Brain*, *145*(5), 1743–1756. https://doi.org/10.1093/brain/awab440

Rey, N. L., Bousset, L., George, S., Madaj, Z., Meyerdirk, L., Schulz, E., Steiner, J. A., Melki, R., & Brundin, P. (2019). α-Synuclein conformational strains spread, seed and target neuronal cells differentially after injection into the olfactory bulb. *Acta Neuropathologica Communications*, *7*(1), 221. https://doi.org/10.1186/s40478-019-0859-3

Rey, N. L., George, S., Steiner, J. A., Madaj, Z., Luk, K. C., Trojanowski, J. Q., Lee, V. M.-Y., & Brundin, P. (2018). Spread of aggregates after olfactory bulb injection of α-synuclein fibrils is associated with early neuronal loss and is reduced long term. *Acta Neuropathologica*, *135*(1), 65–83. https://doi.org/10.1007/s00401-017-1792-9

Rey, N. L., Steiner, J. A., Maroof, N., Luk, K. C., Madaj, Z., Trojanowski, J. Q., Lee, V. M.-Y., & Brundin, P. (2016). Widespread transneuronal propagation of α-synucleinopathy triggered in olfactory bulb mimics prodromal Parkinson's disease. *Journal of Experimental Medicine*, *213*(9), 1759–1778. https://doi.org/10.1084/jem.20160368

Savica, R., Grossardt, B. R., Bower, J. H., Boeve, B. F., Ahlskog, J. E., & Rocca, W. A. (2013). Incidence of Dementia With Lewy Bodies and Parkinson Disease Dementia. *JAMA Neurology*, *70*(11), 1396. https://doi.org/10.1001/jamaneurol.2013.3579

Singh, A., Cole, R. C., Espinoza, A. I., Evans, A., Cao, S., Cavanagh, J. F., & Narayanan, N. S. (2021). Timing variability and midfrontal ~4 Hz rhythms correlate with cognition in Parkinson's disease. *Npj Parkinson's Disease*, *7*(1), 14. https://doi.org/10.1038/s41531-021-00158-x

Souza, R., Bueno, D., Lima, L. B., Muchon, M. J., Gonçalves, L., Donato, J., Shammah-Lagnado, S. J., & Metzger, M. (2022). Top-down projections of the prefrontal cortex to the ventral tegmental area, laterodorsal tegmental nucleus, and median raphe nucleus. *Brain Structure and Function*, *227*(7), 2465–2487. https://doi.org/10.1007/s00429-022-02538-2

Sparkman, N. L., Buchanan, J. B., Heyen, J. R. R., Chen, J., Beverly, J. L., & Johnson, R. W. (2006). Interleukin-6 Facilitates Lipopolysaccharide-Induced Disruption in Working Memory and Expression of Other Proinflammatory Cytokines in Hippocampal Neuronal Cell Layers. *Journal of Neuroscience*, *26*(42), 10709–10716. https://doi.org/10.1523/JNEUROSCI.3376-06.2006

Spiller, J. A., & Keen, J. C. (2006). Hypoactive delirium: Assessing the extent of the problem for inpatient specialist palliative care. *Palliative Medicine*, *20*(1), 17–23. https://doi.org/10.1191/0269216306pm1097oa

Sun, F., Salinas, A. G., Filser, S., Blumenstock, S., Medina□Luque, J., Herms, J., & Sgobio, C. (2022). Impact of α□synuclein spreading on the nigrostriatal dopaminergic pathway depends on the onset of the pathology. *Brain Pathology*, *32*(2). https://doi.org/10.1111/bpa.13036

Tatem, K. S., Quinn, J. L., Phadke, A., Yu, Q., Gordish-Dressman, H., & Nagaraju, K. (2014). Behavioral and Locomotor Measurements Using an Open Field Activity Monitoring System for Skeletal Muscle Diseases. *Journal of Visualized Experiments*, *91*, 51785. https://doi.org/10.3791/51785

Uemura, N., Ueda, J., Yoshihara, T., Ikuno, M., Uemura, M. T., Yamakado, H., Asano, M., Trojanowski, J. Q., & Takahashi, R. (2021). A Synuclein Spread from Olfactory Bulb Causes Hyposmia, Anxiety, and Memory Loss in BAC *SNCA* Mice. *Movement Disorders*, *36*(9), 2036–2047. https://doi.org/10.1002/mds.28512

Van Den Eeden, S. K. (2003). Incidence of Parkinson's Disease: Variation by Age, Gender, and Race/Ethnicity. *American Journal of Epidemiology*, *157*(>11), 1015–1022. https://doi.org/10.1093/aje/kwg068

Volpicelli-Daley, L. A., Luk, K. C., Patel, T. P., Tanik, S. A., Riddle, D. M., Stieber, A., Meaney, D. F., Trojanowski, J. Q., & Lee, V. M.-Y. (2011). Exogenous α-Synuclein Fibrils Induce Lewy Body Pathology Leading to Synaptic Dysfunction and Neuron Death. *Neuron*, *72*(1), 57–71. https://doi.org/10.1016/j.neuron.2011.08.033

Weber, M. A., Sivakumar, K., Tabakovic, E. E., Oya, M., Aldridge, G. M., Zhang, Q., Simmering, J. E., & Narayanan, N. S. (2022). Glycolysis-enhancing α_1-adrenergic antagonists modify cognitive symptoms related to Parkinson's disease. *MedRxiv*, 2022.07.01.22277111. https://doi.org/10.1101/2022.07.01.22277111

Wooten, G. F. (2004). Are men at greater risk for Parkinson's disease than women? *Journal of Neurology, Neurosurgery & Psychiatry*, *75*(4), 637–639. https://doi.org/10.1136/jnnp.2003.020982

Zhang, Q., Abdelmotilib, H., Larson, T., Keomanivong, C., Conlon, M., Aldridge, G. M., & Narayanan, N. S. (2021). Cortical alpha-synuclein preformed fibrils do not affect interval timing in mice. *Neuroscience Letters*, *765*, 136273. https://doi.org/10.1016/j.neulet.2021.136273

Zhang, Q., Aldridge, G. M., Narayanan, N. S., Anderson, S. W., & Uc, E. Y. (2020). Approach to Cognitive Impairment in Parkinson's Disease. *Neurotherapeutics*, *17*(4), 1495–1510. https://doi.org/10.1007/s13311-020-00963-x

FIGURES

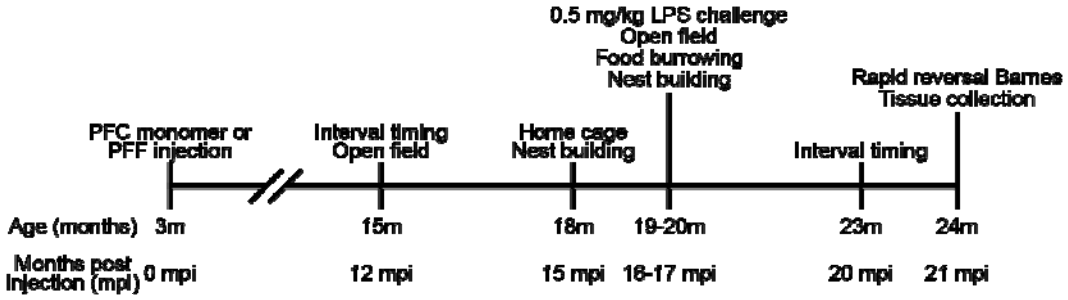

Figure 1. Experimental timeline.

Figure 2. Evaluation of pathology in monomer control and PFF injected mice. A) Top: representative images across the entire rostral-caudal aspect of the brain in two mice treated with PFFs (one saline and

one LPS treated at 16 mpi). Bottom: representative images of two monomer control mice (one saline and one LPS treated at 16 mpi). Semi-quantitative scores of p-syn positive **C)** somas and **D)** neurites of 25 brain regions, with each column representing an individual mouse, averaged over the entire rostral-caudal extent for each brain region examined. Neurites for monomer mice are not displayed as there were zero p-syn positive neurites in any region of any mouse. **E)** Confocal images showing examples of fibrillar pathology in multiple brain regions from PFF injected mice (panels 1–4). Monomer mice showed rare p-syn positive puncta, without clear fibrillar morphology (panel 5). No fibrillar or neurite pathology was found in monomer mice using confocal microscopy. **F)** Averaged semi-quantitative score of pathological α-syn within subregions of the striatum restricted to 0–1.7 mm bregma. **G)** Tyrosine hydroxylase intensity (arbitrary units) from 4 different brain regions PFF treated mice. All data are expressed as mean ± SEM, and each dot represents a single mouse. * $p < 0.05$, ** $p < 0.01$, **** $p < 0.0001$

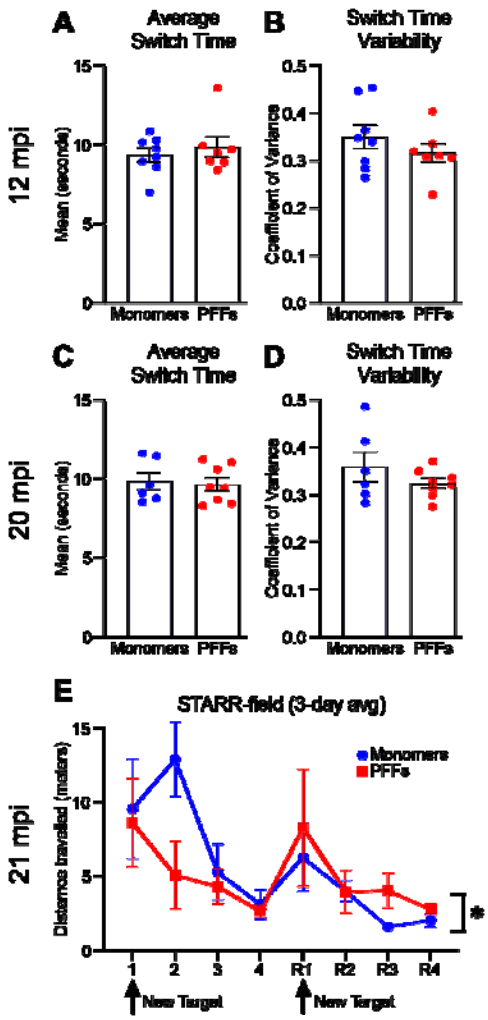

Figure 3. Interval timing and reversal learning in monomer control and PFC PFF mice. A) Mean switch time and **B)** switch time coefficient of variance during the interval timing task at 12 mpi. Data from 8 monomer (blue) and 7 PFF (red) mice. **C)** Mean switch time and **D)** switch time coefficient of variance during the interval timing task. Data from 6 monomer (blue) and 6 PFF (red) mice. **E)** Average total distance travelled averaged across three-days of the rapid reversal Barnes maze. Data from 6 monomer (blue) and 6 PFF (red) mice. All data are expressed as mean ± SEM, and each dot represents a single mouse. Main effect of trial and trial × treatment interaction. * $p < 0.05$

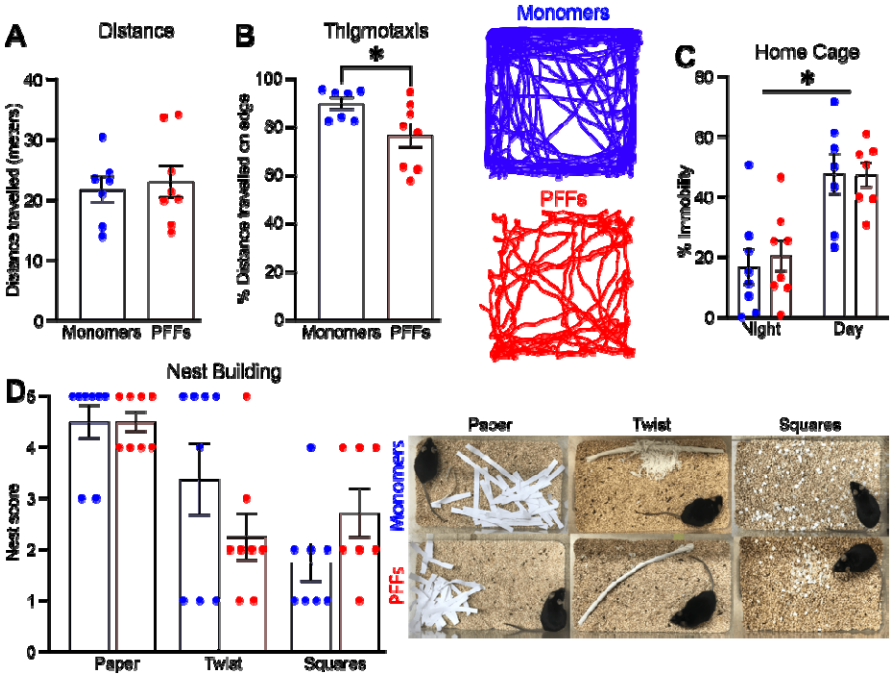

Figure 4. Open field, home cage activity, and nest building in monomer control and PFC PFF mice at 12 mpi. A) Distance travelled and **B)** thigmotaxis during the open field test. The right panel is an example trace from one monomer and one PFF mouse during the open field assay. **C)** Percent immobility time between ~2–3 am (night) and ~6–7 am (morning). **D)** Nest building score for three different materials (shredded paper, cotton twist, and precut cotton squares) with representative images from each material shown in the right panel. Data from 7-8 monomer (blue) and 7-8 PFF (red) mice. All data are expressed as mean ± SEM, and each dot represents a single mouse. * $p < 0.05$

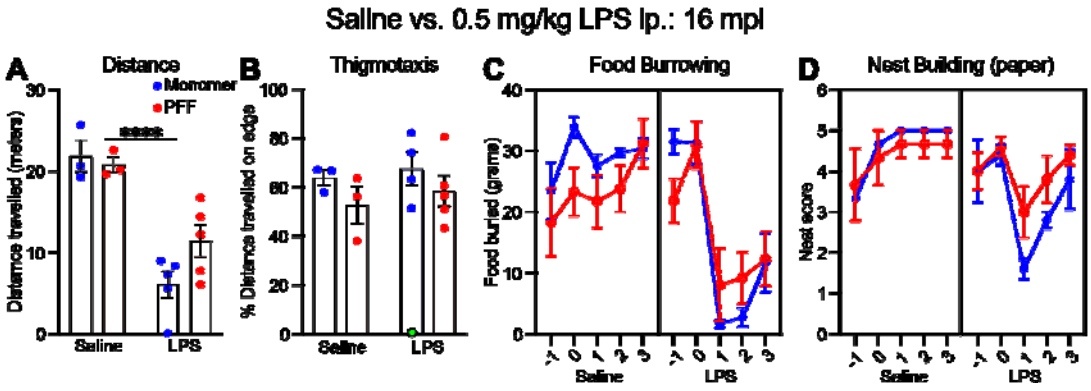

Figure 5. Open field, food burrowing, and nest building during 0.5 mg/kg LPS challenge. A) Distance travelled and **B)** thigmotaxis during the open field after either saline of lipopolysaccharide (LPS) injection. One monomer mouse treated with LPS was excluded from thigmotaxis analysis as no movement was recorded during the assay. **C)** Amount of food buried (in grams) during the food burrowing assay and **D)** nest building score (shredded paper only) for 2 days before and 3 days after either saline or LPS injection. All data are expressed as mean ± SEM, and each dot represents a single mouse. **** $p < 0.0001$

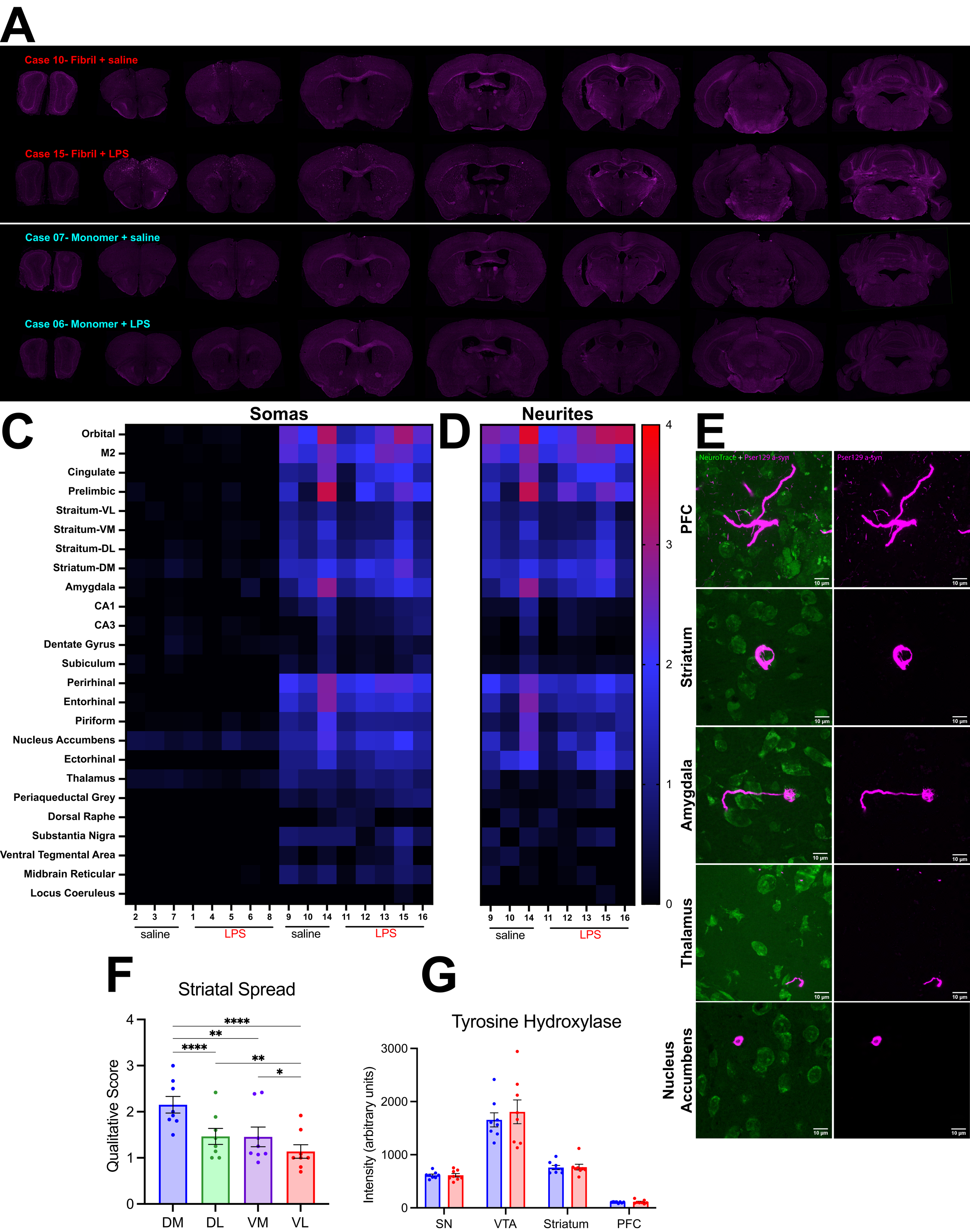
A
Case 10- Fibril + saline
Case 15- Fibril + LPS
Case 07- Monomer + saline
Case 06- Monomer + LPS
C
Somas
Orbital
M2
Cingulate
Prelimbic
Straitum-VL
Straitum-VM
Straitum-DL
Striatum-DM
Amygdala
CA1
CA3
Dentate Gyrus
Subiculum
Perirhinal
Entorhinal
Piriform
Nucleus Accumbens
Ectorhinal
Thalamus
Periaqueductal Grey
Dorsal Raphe
Substantia Nigra
Ventral Tegmental Area
Midbrain Reticular
Locus Coeruleus
2 3 7 1 4 5 6 8 9 10 14 11 12 13 15 16
saline
LPS
saline
LPS
D
Neurites
9 10 14 11 12 13 15 16
saline
LPS
4
3
2
1
0
E
PFC
Striatum
Amygdala
Thalamus
Nucleus Accumbens
NeuroTrace + Pser129 a-syn
Pser129 a-syn
10 µm
F
Striatal Spread
Qualitative Score
4
3
2
1
0
****
**
****
**
*
DM
DL
VM
VL
G
Tyrosine Hydroxylase
Intensity (arbitrary units)
3000
2000
1000
0
SN
VTA
Striatum
PFC